Green Chemistry

Production of Renewable Alcohols from Maple Wood using Supercritical Methanol Hydrodeoxygenation in a Semi-continuous Flowthrough Reactor

Journal:	*Green Chemistry*
Manuscript ID	GC-ART-09-2020-003218.R1
Article Type:	Paper
Date Submitted by the Author:	03-Nov-2020
Complete List of Authors:	Galebach, Peter; University of Wisconsin, Chemical and Biological Engineering Soeherman, Jimmy; University of Wisconsin, Chemical and Biological Engineering Gilcher, Elise; University of Wisconsin, Chemical and Biological Engineering Wittrig, Ashley; ExxonMobil Research and Engineering Company Annandale Johnson, Jillian; ExxonMobil Research and Engineering Company Fredriksen, Thomas; ExxonMobil Research and Engineering Company Wang, Chengrong; ExxonMobil Research and Engineering Company Annandale Lanci, Michael; ExxonMobil Research and Engineering Company Annandale Dumesic, James; University of Wisconsin Madison, Chemical and Biological Engineering Huber, George; University of Wisconsin, Chemical and Biological Engineering

Production of Renewable Alcohols from Maple Wood using Supercritical Methanol Hydrodeoxygenation in a Semi-continuous Flowthrough Reactor

Authors: Peter H. Galebach[†], Jimmy K. Soeherman[†], Elise Gilcher[†], Ashley M. Wittrig[‡], Jillian Johnson[‡], Thomas Fredriksen[‡], Chengrong Wang[‡], Michael P. Lanci[‡], James A. Dumesic[†], George W. Huber[†]

[†]Department of Chemical and Biological Engineering, University of Wisconsin, 1415 Engineering Drive, Madison, Wisconsin 53706, United States.

[‡]ExxonMobil Research and Engineering, 3545 Route 22 East Clinton Township, Annandale, NJ 08801, United States.

Abstract:

Biomass conversion to alcohols using supercritical methanol depolymerization and hydrodeoxygenation (SCM-DHO) with CuMgAl mixed metal oxide is a promising process for biofuel production. We demonstrate how maple wood can be converted at high weight loadings and product concentrations in a batch and a semi-continuous reactor to a mixture of C_2-C_{10} linear and cyclic alcohols. Maple wood was solubilized semi-continuously in supercritical methanol and then converted to a mixture of C_2-C_9 alcohols and aromatics over a packed bed of $CuMgAlO_x$ catalyst. Up to 95 wt% of maple wood can be solubilized in the methanol by using four temperature holds at 190, 230, 300, and 330°C. Lignin was solubilized at 190 and 230°C to a mixture of monomers, dimers, and trimers while hemicellulose and cellulose solubilized at 300 and 330°C to a mixture of oligomeric sugars and liquefaction products. The hemicellulose, cellulose, and lignin were converted to C_2-C_{10} alcohol fuel precursors over a packed bed of $CuMgAlO_x$ catalyst with

70-80% carbon yield of the entire maple wood. The methanol reforming activity of the catalyst decreased by 25% over four beds of biomass, which corresponds to 5 turnovers for the catalyst, but was regenerable after calcination and reduction. In batch reactions, maple wood was converted at 10 wt% in methanol with 93% carbon yield to liquid products. The product concentration can be increased to 20 wt% by partially replacing the methanol with liquid products. The yield of alcohols in the semi-continuous reactor was approximately 30% lower than in batch reactions likely due to degradation of lignin and cellulose during solubilization. These results show that solubilization of whole biomass can be separated from catalytic conversion of the intermediates while still achieving a high yield of products. However, close contact of the catalyst and the biomass during solubilization is critical to achieve the highest yields and concentration of products.

Introduction:

Lignocellulosic biomass (composed of cellulose, hemicellulose, and lignin biopolymers) is a potential source of renewable carbon that could be used to reduce emissions from fossil sources[1]. Research has focused on ways to convert biomass to fuels or chemicals through biological or thermochemical methods similar to what is used in industry[1-4]. Processing biomass often involves numerous, expensive pretreatment steps to separate the biomass into the constituent biopolymers with each step often requiring different reaction conditions and catalysts[5]. Degradation reactions during this pretreatment can hinder downstream processing by producing recalcitrant lignin and cellulose streams that are more difficult to convert than the native biomass[6, 7]. Recent advances in catalytic routes of biomass conversion have demonstrated high yields by using a catalyst during the initial fractionation to stabilize reactive intermediates[6, 8-12]. A promising route for whole lignocellulose conversion which was first demonstrated by the Ford group is conversion of biomass in supercritical methanol with a hydrodeoxygenation catalyst.[13] This

process achieves high yields of alcohols (up to 121 wt% from incorporation of methanol) in a small scale batch system with a high selectivity to alcohols and a low selectivity to side products such as light gases (CO, CO_2, CH_4) and char.[13] An additional advantage of this approach is that the products are primarily alcohols which can undergo further upgrading reactions to the more desired middle distillate range[14, 15].

Research into SCM-DHDO of cellulose, lignin and whole biomass has expanded since the initial work by the Ford group with the reported research only occurring in small batch reactors[16-20]. Yin et al. studied conversion of the sugar fraction of pyrolysis oil to a mixture of single alcohols, diols, and esters over $CuMgAlO_x$[16]. Wu et al. converted cellulose to a mixture of C4-C7 alcohols in supercritical methanol using Cu/ZnO with varying metal oxide additives[17]. Barrett et al. produced aromatic monomers from poplar organsolv lignin using $CuMgAlO_x$ metal oxides in a mixed dimethyl carbonate/supercritical methanol system[18]. Huang et al. studied conversion of soda lignin in supercritical ethanol and methanol using a similar Cu metal oxide catalyst[19]. Previous research in our group has examined the reaction pathways from cellulose and lignin to alcohols in this system shown in Scheme 1[21-23]. Lignin is converted into C_8-C_{10} cyclic alcohols by depolymerization followed by hydrogenation. Cellulose undergoes depolymerization and retro alcohol condensation to smaller oxygenates. These smaller oxygenates then undergo a series of C-C coupling, C-C scission and C-O scission reactions to form C_2-C_7 alcohols. Methanol is reformed to CO and H_2 under the reaction conditions to provide reducing equivalents for hydrogenation. The small batch reactors used in these previous studies are not scalable. Therefore, it is questionable whether SCM-DHDO technology can be scaled to a continuous industrial reactor.

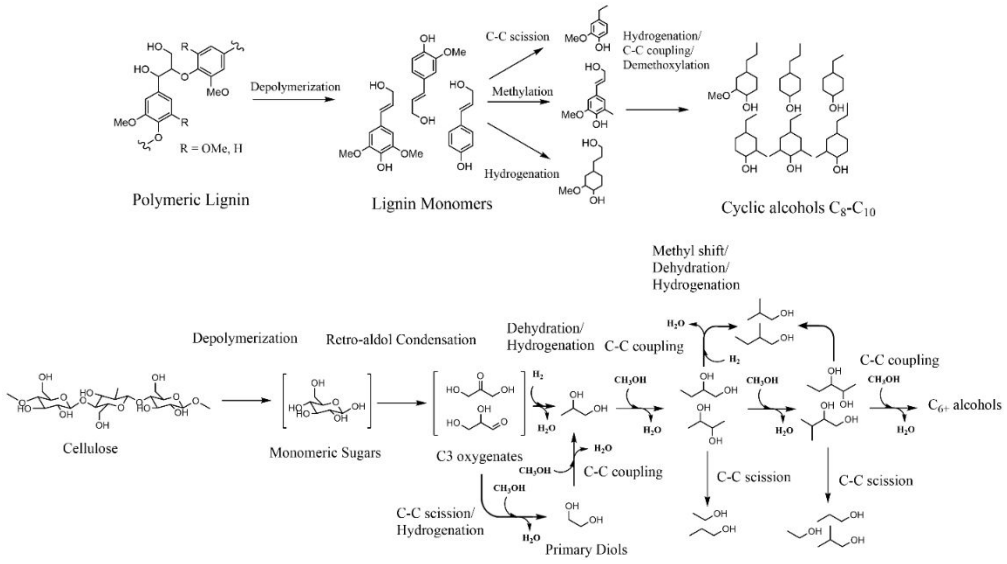

Scheme 1. Conversion pathways for lignin and cellulose to single alcohols in SCM-DHDO (adapted from McClelland et al. and Galebach et al.)

At commercial scales biomass could be introduced continuously by either pumping a biomass slurry or by extrusion of biomass[24, 25]. However, these systems require wide flow paths and fast superficial velocity to prevent bridging and plugging of biomass making them more amenable to larger scales. Several researchers have reported on the use of continuous flow reactors at laboratory scale to study biomass solubilization. Anderson et al. produced stable lignin monomers in 18 wt% yield in a two bed flowthrough system that combined solubilization of lignin from poplar with hydrogenolysis using Ni/C[12, 26]. This system allows decoupling of the solubilization and catalytic steps as well as providing a means to feed real biomass feedstocks over a catalyst in a semi-continuous system that better approximates industrial operation. Depolymerization of lignin is thought to occur through solvolysis of the β-O-4 ether bond via nucleophilic substitution of the hydroxyl group on the C_α of a lignin monomer with a methoxyl group which allows facile C_β-O cleavage.[27, 28] The unsaturated intermediates are then stabilized through hydrogenation. Solubilization of aspen in supercritical methanol has also been

investigated in flow systems by Poirer et al. who were able to solubilize 94% of the wood at 350°C and 172 bar.[29] Cellulose and lignocellulosic biomass solubilization has been investigated with a number of supercritical alcohols and solvents[30-36]. In supercritical methanol cellulose is depolymerized through solvolysis into methylated monomeric and oligomeric sugars.[30] In sub-critical and supercritical water sugars degrade to 5-hydroxymethyl-furfural (HMF) through dehydration or to C_2-C_3 aldehydes and ketones through retro-aldol condensation[37, 38]. Sugars from solvolysis also undergo degradation reactions but at lower rates than during hydrolysis.[39, 40]

Building on this previous research and our research on continuous conversion of glycerol via SCM-DHDO[41] we combined an initial solubilization step of maple wood with a packed bed reactor of $CuMgAlO_x$ catalyst to convert whole biomass in a single reaction step shown in Figure 1. This system can provide insight into the challenges in continuous operation of SCM-DHDO and how this process might be scaled to industrially relevant sizes. In this study NMR and mass spectroscopy were used to characterize the solubilized species from maple wood. The products from the cellulose, hemicellulose and lignin were then characterized after conversion over CuMgAlOx catalyst. The impact of whole biomass on catalyst stability was studied by characterizing the catalyst after converting multiple beds of maple wood.

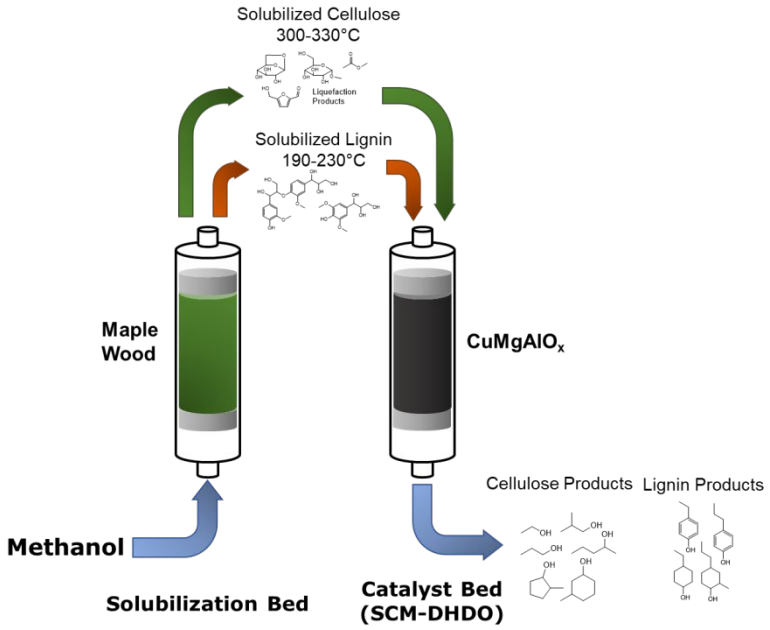

Figure 1. Combined solubilization and catalysis of maple wood to alcohols in a semi-continuous flowthrough reactor.

Experimental Setup and Methods

Feedstock

Maple wood was used as the biomass feedstock. The ash, hemicellulose, cellulose, and lignin content were measured using the procedure to determine structural carbohydrate and lignin composition established by the National Renewable Energy Laboratory (NREL).[42] The maple wood was ground and sieved between 45 and 80 mesh size before use. Yields were based on the carbon in the hemicellulose, cellulose, and lignin fractions of the maple wood. The maple wood was not washed or dried before use and contained approximately 8 wt% moisture.

Semi-continuous solubilization system

The maple wood was solubilized in the setup shown in the supplemental section in Figure S1. Methanol was passed through a ¼" or 3/8" stainless steel tube packed with maple wood using

an HPLC pump (Eldex - SLA1). The tube was heated to 330°C using an aluminum heating block wrapped in heating tape. Sample was collected in a vessel that was kept at room temperature and 2000 psi. The pressure in the collection vessel was maintained with N_2 from a cylinder. As the collection vessel was filled, a small amount of gas was bled from the system via a needle valve to maintain a constant pressure during the run. When samples were taken, additional N_2 was added to the collection vessel to maintain a constant pressure. Samples were collected every 15 to 30 minutes. During startup the maple wood bed was first heated to 120°C then rapidly heated to the desired solubilization temperature at 10°C min^{-1}. Methanol was introduced into the bed at the start of the 10°C min^{-1} temperature ramp. The start of each run was counted as the time the solubilization bed reached the desired temperature. The mass of solubilized biomass was calculated by unloading the bed after each run and measuring the mass lost. The composition of the maple wood after solubilization was measured using Thermogravimetric analysis (TGA).

Combined semi-continuous solubilization and packed bed reactor system

In our previous research we constructed a continuous reactor with a bed of $CuMgAlO_x$ catalyst to convert glycerol as a model compound for cellulose[41]. The continuous reactor from that work was combined with the semi-continuous solubilization system to convert maple wood semi-continuously in the setup shown in Figure 2. The solubilization bed was composed of 3/8" tubing filled with 1.87g of maple wood with a 2-inch bed of glass beads to preheat the solvent. The bed was held in place by quartz wool (Acros) at the top and bottom of the bed. The bed was heated with an aluminum heating block wrapped with heating tape. Before reaction the bed of maple wood was filled with methanol using an HPLC pump (Eldex – SLA1) to purge the system of any air. The catalyst bed consisted of 1.42g of catalyst with a 0.5-inch preheating zone of glass beads held in place by quartz wool. The catalyst was reduced at 350°C for 4 hours in a 100 mL min^{-1}

stream of H_2 with a 1°C min^{-1} ramp before reaction. The liquid products were collected in a 150 mL collection vessel that was chilled to 0°C while the gases were separated from the liquids and sent to an online GC. The flowrate of gas products was measured periodically with a bubble flowmeter. To replace a bed of maple wood the system was cooled to room temperature and lowered to atmospheric pressure. A small flow of H_2 was kept going to the catalyst bed to maintain an inert atmosphere and prevent oxidation. The spent bed of maple wood was then removed, and a fresh bed of maple wood was added to the system. The bed of maple wood was then filled with methanol to displace any air in the bed. The catalyst was observed to synthesize a small amount of higher alcohols during reaction. To account for these alcohols, pure methanol was fed to the catalyst bed before and after reaction to measure the yield of higher alcohols in a blank reaction which were subtracted from the total carbon yield.

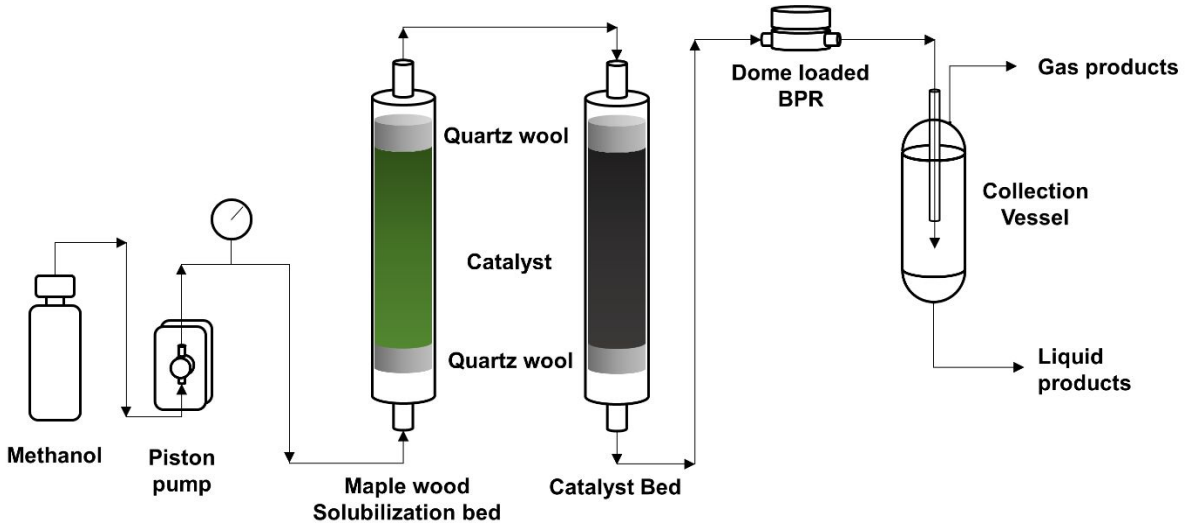

Figure 2. Semi-continuous solubilization and SCM-DHDO reactor for converting maple wood at high pressure and temperature in supercritical methanol with CuMgAl oxide. Reactor Conditions: SCM-DHDO reactor: 300°C, 2000 psig, 1.42 g $CuMgAlO_x$, 0.431 mL/min MeOH.

Batch reactor system

Batch reactors were built using Swagelok unions and bleed valves as described in our previous work[21, 43] The batch reactors were heated in a fluidized sand bath to 300°C in approximately 5 minutes. The reaction was stopped by quenching the batch reactors in water. Gas samples were collected in an inverted water cylinder and analyzed with GC. Liquid samples were collected from the opened reactors using a syringe. Liquid samples were filtered using a 0.22 μm filter and analyzed by GC.

Catalyst synthesis and regeneration

The catalyst was synthesized by co-precipitation of a solution of $NaCO_3$ with a solution containing Cu, Mg, Al nitrates in a molar proportion of $Cu_3Mg_{12}Al_5$ similar to previous research[43-45]. The Cu, Mg, Al solution was added to the solution of $NaCO_3$ with a syringe pump such that the solution was completed added in 1 h. A solution of NaOH was cofed with a syringe pump to maintain the $NaCO_3$ solution at a pH of 10 during synthesis. The solution was then aged at 60°C for 24 h and then filtered and washed. The resultant hydrotalcite was dried in an oven overnight at 110°C. The dried hydrotalcite was crushed and stored as a hydrotalcite. Before a reaction the hydrotalcite precursor was calcined at 460°C for 12 h at 5°C min^{-1}.

The catalyst was regenerated in the semi-continuous reactor by removing the catalyst from the catalyst bed and calcining ex-situ at 460°C for 4 hours with a 1°C min^{-1} ramp in a furnace. The catalyst was then reloaded into the reactor and reduced in-situ at the same conditions as during startup.

Product Analysis

Gas products were analyzed with a Shimadzu GC-2014 equipped with a 30m RT-Q-Bond column and flame ionization (FID) and thermal conductivity (TCD) detectors using He carrier gas.

The GC oven was held at 40°C for 5 minutes then ramped to 150°C at 5°C min^{-1} and held for 11 minutes. Liquid products were analyzed by FID using a Shimadzu GC-2010 equipped with an RTX-VMS column, by GC MS using a Shimadzu GCMS-QP2010 mass spectrometer equipped with an RTX-VMS column. The GC FID oven was held at 40°C for 5 minutes then ramped to 240°C at 7.5°C min^{-1} and held for 15 minutes. Response factors were calibrated using known standards. For compounds without available standards, effective carbon number was used instead. For the C_6-C_7 cyclic alcohols and C_8-C_{10} cyclic alcohols the response factor for cyclohexanol was used. For the phenolics the response factor for isoeugenol was used.

Fourier Transform Ion Cyclotron Resonance Mass Spectroscopy (FT-ICR MS)

All experiments were performed using a Bruker solariX FT-ICR MS with an actively shielded 15T superconducting magnet. The acquisition software was "ftmsControl" (version 2.2.0, Bruker Daltonics). Data was viewed and calibrated using "Bruker Compass Data Analysis" (version 5.0.203, Bruker Daltonics). Each sample was acquired through two different ionization mechanisms: Atmospheric Pressure Chemical Ionization (APCI) and Atmospheric Pressure Photo-Ionization (APPI), both in positive ion mode. In all experiments, samples were diluted 25 times by volume in a blend of methanol and toluene (at a volumetric mixture ratio of 9:1, methanol:toluene). Ion accumulation time was between 0.025 and 0.060 seconds, adjusted for response. An 8MW time domain date set size was used, with an average resolving power of approximately 580,000 at *m/z* 400. Mass range for analysis was between *m/z* 100 and 3000. 200 scans were collected and averaged together in all experiments.

APCI

Select instrument parameters for APCI were as follows: sample solution was infused using the system's integrated syringe pump into the mass spectrometer at a flow rate of 5.0 uL/hr. The vaporizing temperature was 370 ºC, the corona needle current (used in APCI mode only) was 1000 nA, the nebulizer gas pressure was 2.0 bar, and dry gas flow was 3.4 L/min, with nitrogen as the drying gas, and the dry gas temperature was 200 ºC. Capillary voltage was 2700 V, and the spray shield (capillary end plate offset) was -600 V. Funnel RF amplitude was 100 Vpp. The time of flight to detector was set to 0.900 ms. Excitation energy was ramped linearly from 14.0% to 55.0% (relative to effectible maximum), over the full length of acquisition (76.7 to 2500 kHz).

APPI

Certain different values were used in APPI to demonstrated better response, or to correct for peak splitting, or to achieve a more stable sample spray, and are described below (all values listed above and not herein were kept the same). Syringe flow rate was 3.0 uL/hr. The vaporizing temperature was 400 ºC. The nebulizer gas pressure was 1.2 bar. The drying gas flow was 3.9 L/min. Capillary voltage was 2400 V, and the spray shield was -500 V. Funnel RF amplitude was 150 Vpp. Time of flight was 0.750 ms. Excitation energy was ramped from 8.0% to 19.0% at the transition mass, then to 55.0% up to the end frequency of excitation. The transition mass was *m/z* 1000.0.

Data was internally calibrated using a homologous series and then exported to a table with mass and intensity. Background and noise peaks that do not fall into a Kendrick mass defect series were removed from the data sets. Exported peaks were then imported into PetroOrg S-10.2 software for elemental formula assignment.[46] Data composition is visualized with internal software.

Gel permeation chromatography

Analytical GPC was performed on a Shimadzu LC20 with a photodiode array detector (SPD-M20A). Separation was performed using two PSS PolarSil linear S columns (7.8 mm × 30 cm, 5μm) in series. For each analysis, a 1 μl sample containing 1 mg mL^{-1} lignin or reaction product was injected. The mobile phase was 0.1 M lithium bromide (LiBr) in *N*,*N*-dimethylformamide (DMF) at 40 °C and a flow rate of 0.3 mL min^{-1}. The molecular weight distribution was calibrated at λ = 280 nm using Polystyrene ReadyCal Standard Set M(p) 250–70 000 Da (P/N 76552; Fluka, Sigma/Aldrich, St Louis, MO, USA).

Characterization of products with NMR

The products from the solubilization and semi-continuous reactor systems were characterized by quantitative ^{13}C and 2D HSQC NMR. Samples were dissolved in DMSO-d_6 and pyridine-d_5 to produce a solution of 10 wt% sample, 72 wt% DMSO-d_6, and 18 wt% pyridine-d_5. The quantitative ^{13}C NMR experiments were acquired on a Bruker Biospin (Billerica, MA) AVANCE III 500 MHz spectrometer fitted with a DCH (^{13}C-optimized) cryoprobe using the standard Bruker pulse sequence "zgig30" with an inter-scan relaxation delay of 15 s, a sweep width of 240 ppm, O1P at 110 ppm, TD of 59520 with an acquisition time of 1 s, and 512 scans. The quantitative ^{13}C NMR experiments were analyzed with MestraNova software with the DMSO solvent peak as the internal reference at 39.50 ppm. The 2D HSQC NMR experiments were carried out on a Bruker Biospin (Billerica, MA) AVANCE 600 MHz spectrometer fitted with a cryogenically cooled 5 mm TXI gradient probe. The standard Bruker pulse sequences "hsqcedetgpsisp2p3" and "hmbcetgpl3nd" were used with an inter-scan relaxation delay of 2 s, 8 scans, sweep widths of 220 ppm in F1 and 12 ppm in F2, O1P of 110 ppm in F1 and 5.5 ppm in F2, and TD of 3366 in F1 and 1000 in F2 for a total of 5 h per experiment. Bruker's Topspin 3.5

software was used to process spectra. The DMSO solvent peak was used as internal reference (δ_C /δ_H: 39.50/2.49).

Equations

$$\%\ \boldsymbol{Biomass\ Solubilized} = \frac{\boldsymbol{Residual\ maple\ wood\ after\ reaction}}{\boldsymbol{Mass\ of\ maple\ wood\ loaded\ in\ bed}} \quad \text{Eqn. 1}$$

$$\boldsymbol{Carbon\ yield} = \frac{\boldsymbol{mmol\ C_{identified\ liquid\ products}}}{\boldsymbol{mmol\ C_{feed} \cdot \%\ of\ GC\ area\ identified}} - \boldsymbol{mmol\ C_{HAS\ products}} \quad \text{Eqn. 2}$$

$$\boldsymbol{Holocellulose\ yield} = \frac{\boldsymbol{mmol\ C_{C2-C6\ alcohols,\ C6-C7\ cyclic\ alcohols,\ esters,\ ethers,\ unspecified}}}{\boldsymbol{mmol\ C_{cellulose+hemicellulose\ in\ feed}}} \quad \text{Eqn. 3}$$

$$\boldsymbol{Lignin\ yield} = \frac{\boldsymbol{mmol\ C_{C8-C10\ cyclic\ alcohols,\ phenolics,\ dimers}}}{\boldsymbol{mmol\ C_{lignin\ in\ feed}}} \quad \text{Eqn. 4}$$

$$\boldsymbol{High\ boiling\ yield} = \boldsymbol{mmol\ C_{C_8-C_{10}\ cyclic\ alcohols+phenolics}} \cdot \frac{\boldsymbol{area\ of\ monomers\ in\ HT\ GC}}{\boldsymbol{area\ of\ dimers+trimers\ in\ HT\ GC}}$$

Eqn. 5

Catalyst characterization

Catalysts were characterized using multiple techniques. The surface area of the catalysts was measured before and after reaction with N_2 physisorption using an ASAP 2020 (micromeritics). The fresh and spent catalysts were calcined before N_2 physisorption. The surface area of copper sites were measured by oxidizing the Cu sites on the catalyst with N_2O and measuring the amount converted[47]. To oxidize the copper with N_2O we first carried out a temperature programmed reduction (TPR) using calcined catalyst at from 20°C to 350°C with a 1°C min^{-1} ramp and held for 4 hours in 10% H_2/Ar. We measured the effluent gases with a TCD to measure the uptake of H_2 on the catalyst. The catalyst was then cooled to 90°C in pure He and N_2O was pulsed over the catalyst in 0.5 mL pulses. The effluent gases were measured with a mass spectrometer (Cirrus 2 – Micromeritics) to measure the amount of N_2O consumed and N_2 released

by the catalyst. The surface Cu sites were counted by assuming the stoichiometry of equation 6 below.

$Cu^0 + N_2O \rightarrow Cu_2O + N_2$ Eqn. 6

The bulk Cu content of the catalyst was measured using ICP-OES with a Vista-MPX ICP-OSE.

Catalyst characterization by STEM

A particle size distribution analysis was performed using scanning transmission electron microscopy (STEM) imaging on a FEI Titan STEM with Cs aberration correction operated at 200 kV in high-angle annular dark field (HAADF) mode. Samples were prepared by dispersing the passivated catalyst in ethanol and grinding in a mortar to suspend the mixture before depositing the sample onto a holey carbon coated copper grid. All samples were plasma cleaned prior to loading in the microscope.

Results and Discussion:

Solubilization of maple wood in subcritical/supercritical methanol

Maple wood was loaded in a ¼" tubular bed and solubilized by pumping methanol through the bed with a piston pump. The effect of temperature on solubilization of maple wood was first studied by varying the temperature of the solubilization bed between 190 and 330°C and characterizing the residual biomass with thermogravimetric analysis (TGA). The amount of biomass solubilized in each run was measured by unloading the biomass from the reactor and weighing the solids. The amount of maple wood solubilized and composition of the residue at varying temperatures are shown in Table S1 in the SI. The TGA of the maple wood before and after solubilization at varying temperature is shown in Figure 3. TGA of the fresh maple wood has

a large peak at approximately 350°C which corresponds to degradation of cellulose and a shoulder peak from 250-300°C which is likely hemicellulose and lignin.[48] As the temperature of degradation increases less of the biomass is able to be thermally decomposed. Much of the shoulder peak is removed by solubilizing the maple wood at 190°C. After solubilization at 230°C the shoulder peak is completely removed, and the only peak is from cellulose at 350°C. Cellulose is not solubilized until 300°C and is not fully solubilized even after 2 h. All fractions of maple wood are solubilized at 330°C, but 23% of the solids remain as degradation products. To achieve an approximately constant rate of maple wood solubilization and a high amount of solubilization, the maple wood was solubilized at four temperatures with 30-minute holds at 190°C, 230°C, 300°C, and 330°C. Degradation of biomass was minimized by using an appropriate temperature to solubilize each fraction of biomass making it possible to solubilize 86% of the maple wood.

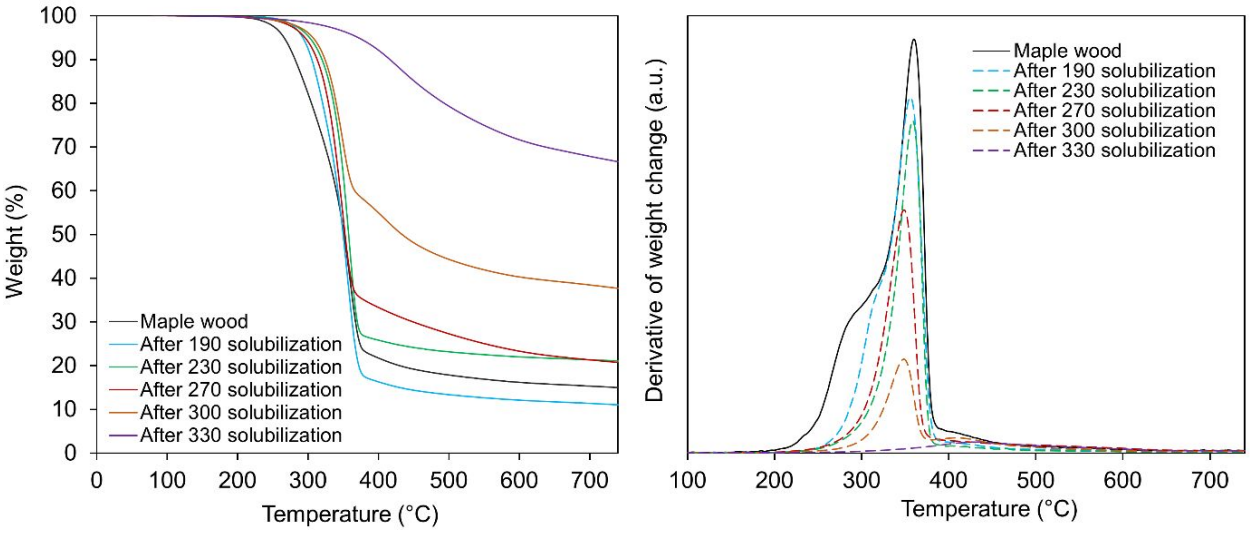

Figure 3. Thermogravimetric analysis (TGA) of fresh maple wood and the maple wood residue after solubilization with supercritical methanol at 190°C, 230°C, 300°C, and 330°C.

The composition of the species solubilized at 190 to 330°C were analyzed with HSQC and quantitative ^{13}C NMR experiments shown in Figure 4 and Table 1 respectively. At 190 and 230°C the HSQC shows correlations that correspond to aryl ether, phenylcourmaran, and resinol linkages

between lignin monomer units in the C-O aliphatic region (δ_C/δ_H 55-95/3-5) showing that lignin is still intact as oligomers after solubilization. The C-O aliphatic region also contains unidentified correlations at δ_C/δ_H of 60-80/3-3.5 which are likely from solubilized oligosaccharides. Correlations in the aromatic region at δ_C/δ_H of 95-165/5-8 ppm show that the lignin monomers are a mixture of syringyl and guaiacyl units with a smaller amount of hydroxyphenols. Integration of the monomer peaks shows that a higher proportion of the monomers at 190°C are guaiacyl (S:G ratio of 0.74) than at 230°C (S:G ratio of 2.57). Anomeric carbons at δ_C/δ_H of 95-105/4-4.5 further suggests a small amount of hemicellulose or cellulose is soluble at the low temperatures.[49] Recondensation of lignin monomer units is difficult to determine via HSQC. The 190°C soluble compounds are composed primarily of aromatic carbons (69%) with smaller amounts of C-O aliphatic (17%) and carbonyl (8%) carbons. The distribution of carbons is consistent with the soluble species being monomeric or oligomeric lignin units where aromatic carbons are from the carbons in the phenol ring while the C-O aliphatic carbons are from either methoxy groups in guaiacol or syringol units or hydroxy carbons on the propyl tail. Carbonyl carbons could be from either a ketone or aldehyde on the propyl tail or from methyl acetate from acetyl groups in the hemicellulose. At 230°C the amount of aromatic carbons decreases to 48% while the C-O aliphatic carbons increase to 38% which may indicate some solubilization of hemicellulose from the biomass. Anomeric carbons from oligosaccharides are included in the aromatic region although they are C-O aliphatic carbons due to a higher downfield shift from being bonded to two oxygens. The HSQC of the soluble species at 300°C contains a few correlations from guaiacol and syringol units from lignin in the aromatic region although most correlations in the aromatic region are unresolved. At 300°C correlations from anomeric carbons at δ_C/δ_H 95-105/4-5.5 ppm are prominent indicating possible solubilization of cellulose. The species solubilized at 300°C and

330°C also have a large number of peaks in the C-O aliphatic region that do not correspond to any lignin linkages but may be from hydroxyl carbons in a polysaccharide.[50] Solubilization of the cellulose fraction also appears to produce degradation products as evidenced by an increase in the number of C-C aliphatic peaks (δ_C/δ_H of 0-55/0-3). Quantitative ^{13}C of the soluble species at 300 and 330°C shows that most carbons are C-O aliphatic (39% and 35% respectively) with lesser amounts of aromatic carbons (28% and 17%) from residual lignin and anomeric carbons. At 330°C, 32% of the carbons are C-C aliphatic possibly from the formation of humins indicating degradation of the cellulose is occurring during solubilization[51].

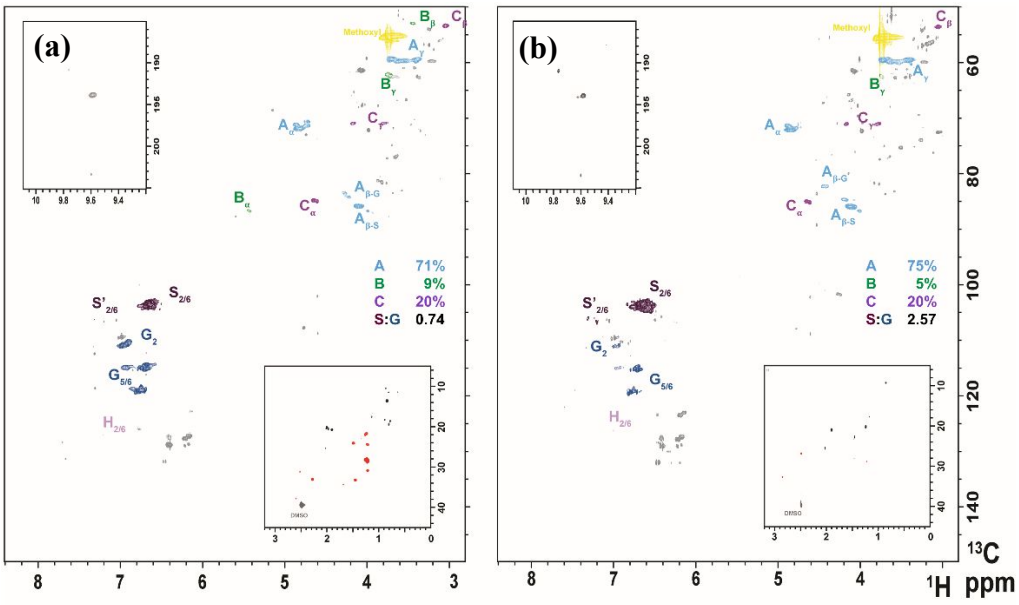

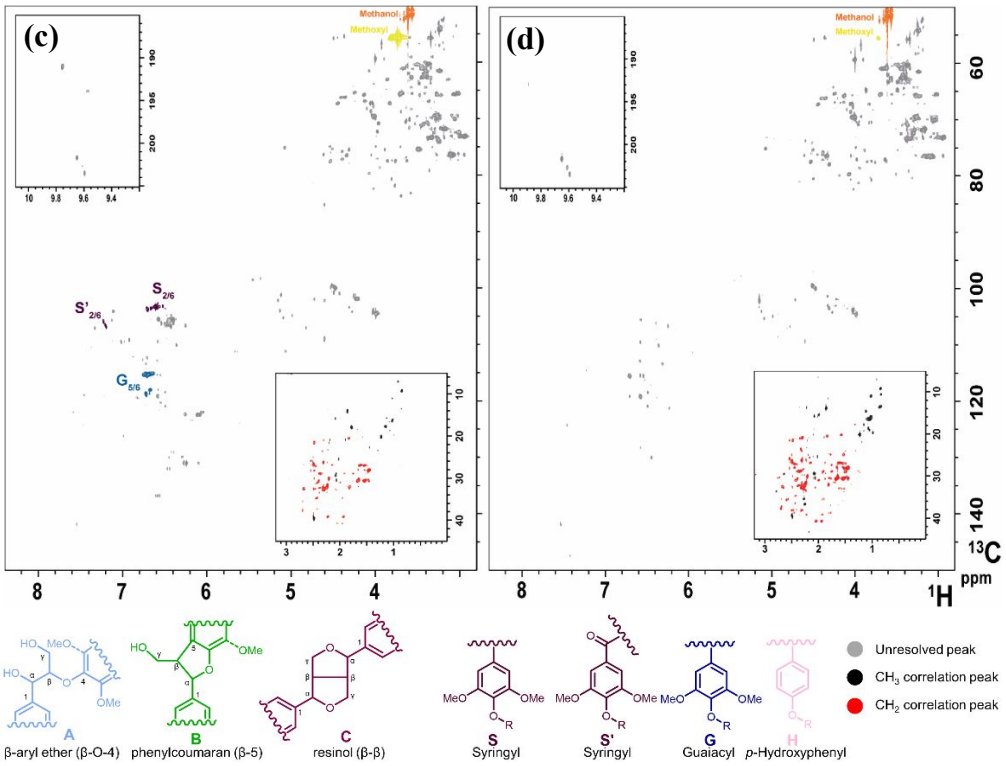

Figure 4. C-O aliphatic and aromatic regions of HSQC of maple wood solubilized in sub-critical and supercritical methanol at 190°C (a), 230°C (b), 300°C (c), 330°C (d). (Carbonyl and C-C aliphatic regions are shown in insets on top-left and bottom-right)

Table 1. C-C aliphatic, C-O aliphatic, aromatic, and carbonyl content from quantitative ^{13}C NMR of maple wood solubilized in subcritical and supercritical methanol at 190, 230, 300, and 330°C.

	% of area in each region from quantitative ^{13}C NMR			
	C-C aliphatic (0-55 ppm)	**C-O aliphatic (55-95 ppm)**	**Aromatic (95-165 ppm)**	**Carbonyl (165-220 ppm)**
Liquids after 190°C	6	17	69	8
Liquids after 230°C	8	38	48	6
Liquids after 300°C	20	39	28	13
Liquids after 330°C	32	35	17	16

The soluble products were further characterized with FT-ICR MS, shown in Figure 5 a-h. Figure 5 shows the oxygen number vs. carbon number as well as the double bond equivalence (DBE) vs. carbon number of the compounds solubilized at 190 to 330°C. A line for where lignin

and cellulose oligomers carbon vs. oxygen and carbon vs. DBE is also shown in Figure 5. The line for lignin is based on an oligomer similar in composition to the S:G ratio and A, B, C linkages from the HSQC in Figure 4. In Figure 5 a-b the main peak is at C 20 to C 22 with 6-8 oxygen and 10-12 DBE which corresponds to a lignin dimer unit. The shoulder of the main peak in Figure 5a with approximately 1-2 fewer oxygens and carbons is likely from varying amounts of methoxy groups on the phenol ring between guaiacyl and syringyl monomer units. The smaller peaks in Figure 5a-b are centered at 11 C, 33 C, and 44 C which correspond to monomers, trimers, and tetramers respectively. The presence of distinct peaks shows the lignin is mostly solubilizing as intact monomers and oligomers rather than recondensing to recalcitrant lignin. The species solubilized at 230°C in Figure 5c-d look nearly identical to the species at 190°C showing that lignin is still the main compound solubilizing at lower temperatures. There is no evidence of oligomeric sugars from hemicellulose in the soluble compounds at 230°C suggesting that either hemicellulose has not solubilized yet or the soluble sugars are not visible with this technique. Small products from hemicellulose such as methyl acetate or furfural would be too small to observe by FT-ICR MS. The compounds solubilized at 300 and 330°C in Figure 5e-h do not have distinct peaks and appear to make a wide distribution of different products. We hypothesize that these products are from liquefaction of hemicellulose and cellulose during solubilization. Similar compounds were observed in reactions with glucose and cellulose using a calcined catalyst that we attributed to recondensation of unstable intermediates during solubilization that form in the absence of an active hydrogenation catalyst[21, 43]. These compounds may also be the source of C-C aliphatic carbons that were observed by NMR.

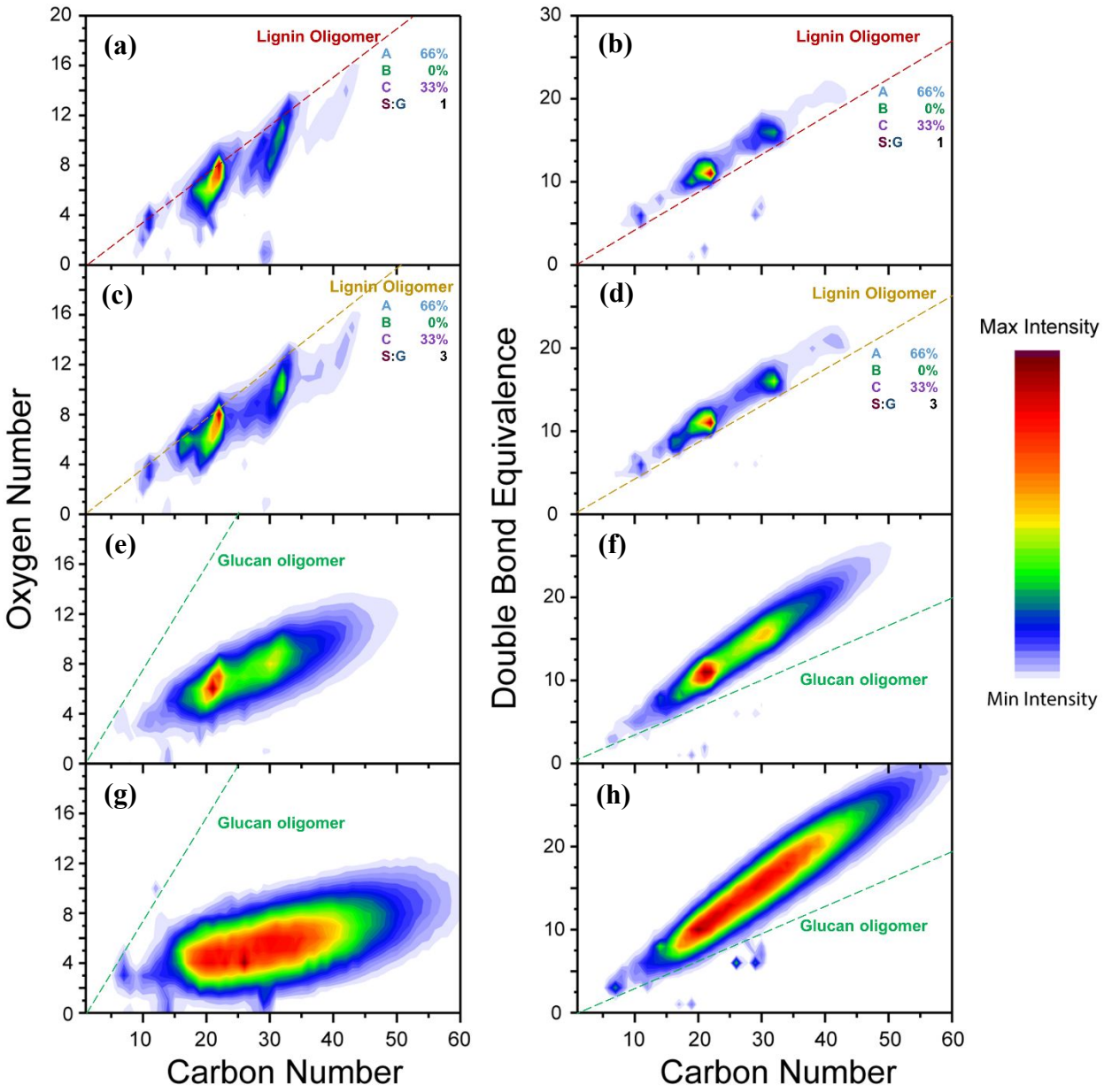

Figure 5. FT-ICR MS of maple wood solubilized in subcritical and supercritical methanol at 190°C (a-b), 230°C (c-d), 300°C (e-f), and 330°C (g-h). Figure shows oxygen content vs. carbon number (a, c, e, g) and double bond equivalents (DBE) vs. carbon number (b, d, f, h) of liquid products.

Semi-continuous conversion of maple wood with catalyst regeneration

We combined the solubilization system with a packed catalyst bed to semi-continuously feed and convert solubilized maple wood to alcohols over $CuMgAlO_x$ as described in the

experimental section. The packed bed of $CuMgAlO_x$ was kept at 300°C while the solubilization bed was operated at 190, 230, 300 and 330°C. The line between the solubilization bed and the packed catalyst bed was kept at the same temperature as the solubilization bed which was found to prevent deposition of soluble lignin in the line. After the consumption of maple wood the reactor was cooled and the bed of maple wood was replaced with a fresh bed. After two beds of maple wood the catalyst was regenerated by calcining and reducing as described in the experimental section. This procedure was repeated for a total of 6 beds of maple wood. The liquid products were sampled at two points during each bed of maple wood. First, after the maple wood was solubilized at 230°C and second, after solubilizing the maple wood at 330°C.

The liquid products after conversion of six beds of maple wood are shown in Table 2. The total carbon yield is approximately 65-75% with most products being C_2-C_6 mono-alcohols and C_6-C_7 cyclic alcohols. The liquid products also contain a mixture of ethers and esters as well as C_8-C_{10} cyclic alcohols and phenolics. The C_2-C_6 mono-alcohols, ethers and esters, and C_2-C_6 unspecified products contain the same products as reactions run with cellulose in batch reactors.[21] The C_8-C_{10} cyclic alcohols and phenolics were previously observed in reactions with extracted lignin in batch reactors.[23] The C_6-C_7 cyclic alcohols are possibly from hydrogenation of intermediates from degradation of cellulose during solubilization. Close GC-MS matches of these compounds are shown in Figure S2 in the SI. The lignin yield was calculated using the carbon of lignin in the maple wood and the yield of products from lignin (C_8-C_{10} cyclic alcohols, phenolics, and dimers). The lignin yield of lignin is approximately 40% to 55% higher 2nd bed after regeneration (2, 4, and 6). The variation in yield is mostly due to increases in the phenolic and dimer yield in the 2nd bed. This may be due to lignin depositing in the catalyst bed and only eluting after longer times on stream. The holocellulose yield was calculated using the carbon of

holocellulose (hemicellulose and cellulose) in the maple wood and the yield of cellulose products. The holocellulose yield is approximately 80-90% with a slight increase in selectivity to C_2-C_6 mono-alcohols after regeneration of the catalyst. The holocellulose yield in this study is similar to our previous studies in semi-batch reactors with unreduced $CuMgAlO_x$ and cellulose but is lower than reactions with reduced $CuMgAlO_x$[22]. The difference is likely due to increased degradation of the cellulose during solubilization. The yield of products are further separated into the products collected from 190-230°C and the products from 300-330°C. The holocellulose products at 190-230°C are mostly methyl acetate and ethanol from conversion of acetyl groups in hemicellulose indicating hemicellulose is solubilizing at these temperatures. However, the lack of additional alcohol products suggests that hemicellulose oligomers are not being converted over the catalyst during solubilization at 190 and 230°C. The total carbon yield from 300-330°C products is much higher than the 190-230°C products (50-60% vs. 11-15%). The 300-330°C products are mostly from holocellulose but there is a large amount of lignin products as well. The high yield of lignin products suggests that lignin monomers and dimers are eluting from the catalyst bed slowly.

Table 2. SCM-DHDO of maple wood in a semi-continuous solubilization and packed bed reactor with six beds of maple wood and catalyst regeneration after Beds 2 and 4. Reaction conditions – solubilization: 190-330°C (10°C min^{-1} ramp) – catalyst: 300°C, 138 bar, 1.87 g maple wood or cellulose, 1.42 g reduced $CuMgAlO_x$ catalyst, 0.43 mL min^{-1} methanol, 20 mL/min H_2.

Liquid Products	Bed 1	Bed 2	Bed 3	Bed 4	Bed 5	Bed 6
Total carbon yield (%C)	67.2	71.5	64.2	72.9	74.6	81.4
Lignin Yield ($\%C_{lignin}$)[a]	44.3	57.3	38.2	52.0	50.5	70.6
Holocellulose yield ($\%C_{holocellulose}$)[b]	81.9	80.5	80.8	86.3	90.0	88.3
Selectivities						
C_2-C_6 mono-alcohols	36.3	31.4	39.5	34.0	33.7	29.0
C_6-C_7 cyclic alcohols	18.6	18.0	18.6	17.6	20.9	16.9
Ethers and esters	8.9	9.3	9.0	10.5	6.7	10.0
Unknown C_2-C_6 alcohols, ethers, and esters[c]	10.6	10.1	9.7	10.1	12.3	10.2
C_8-C_{10} cyclic alcohols	13.2	13.0	11.5	12.0	12.6	10.9
Phenolics	8.3	10.5	7.7	9.7	7.9	8.9
Lignin dimers and trimers	4.2	7.8	3.9	6.1	5.8	14.0
Residual Biomass (wt%)	17.8	10.0	11.4	12.3	9.2	6.2
Unsolubilized cellulose (wt%)	11.6	3.6	5.6	6.0	3.2	1.2
Char and degradation products (wt%)	5.1	4.9	5.2	5.7	5.6	4.3
190-230°C carbon yield (%C)	14.3	14.0	13.7	13.7	12.6	13.9
Lignin yield ($\%C_{lignin}$)	13.2	18.0	12.6	16.1	14.6	19.2
Holocellulose yield ($\%C_{holocellulose}$)	15.0	11.3	14.4	12.2	11.3	10.5
300-330°C carbon yield (%C)	52.9	57.5	50.5	59.7	62.1	67.4
Lignin yield ($\%C_{lignin}$)	31.1	39.2	25.6	37.1	36.0	51.4
Holocellulose yield ($\%C_{holocellulose}$)	66.9	69.2	66.4	74.1	78.8	77.7

[a]mol C from cellulose products/mol C of hemicellulose and cellulose in the maple wood
[b]mol C from lignin products/mol C of lignin in the maple wood
[c]products that are observed in the GC and may be identified in the GC-MS but were not verified by standards

The impact of regenerating the catalyst can be seen in the gaseous products, mostly CO, CO_2, and H_2 produced from methanol reforming (Figure 6). The methanol reformed decreases from bed 1 to bed 2 from 29% to 24%. After calcination and reduction of the catalyst the methanol reformed activity at the start of bed 3 returns to 28% before decreasing to 23% at the end of bed 4. The decrease in methanol reforming activity suggests the catalyst is losing activity possibly due

to deposition of carbon on the catalyst. Previous conversion of glycerol as a model compound in a continuous system showed slower deactivation than what was observed here[41]. However, since the catalyst activity increases after regeneration most of the deactivation is reversible.

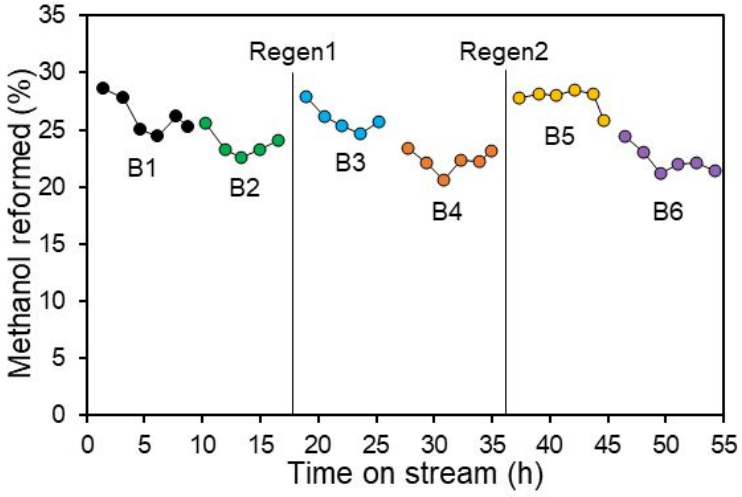

Figure 6. Methanol reformed during SCM-DHDO of maple wood in semi-continuous reactor with catalyst regeneration between beds 2-3 and 4-5.

We also examined the molecular weight of the 190-230°C and 300-330°C products with gel permeation chromatography (GPC), shown in Figure 7. The 190-230°C products have a prominent peak at 170 Da which corresponds to a lignin monomer. There is a second small peak at 270 Da which is likely lignin dimers. The 300-330°C products have a large peak at 270 Da, which may be lignin dimers, and a broad range of molecular weights up to 500 Da. There are more dimers in the second bed of maple wood before regeneration (beds 2, 4, and 6) for both the 190-230°C and 300-330°C products. The GPC of the 300-330°C products doesn't show compounds as high molecular weight as what was observed by FT-ICR MS in Figure 5 (e-h). This suggests that the degradation products from solubilization are catalytically broken down into smaller compounds or deposited on the catalyst.

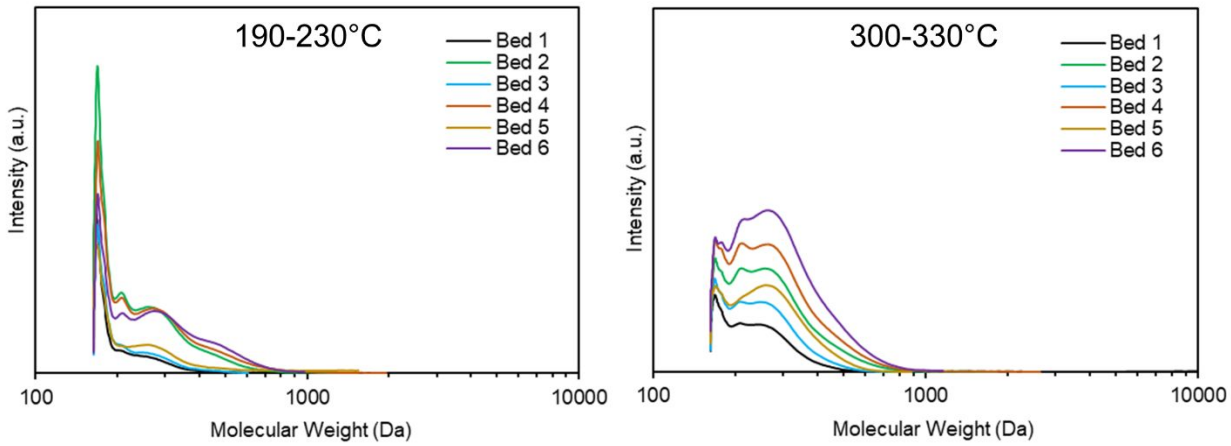

Figure 7. GPC data of 190-230°C and 300-330°C products from SCM-DHDO of maple wood in a semi-continuous solubilization and packed bed reactor.

Solubilization and conversion of maple wood with multi-temperature catalyst bed

We examined conversion of maple wood where the catalyst bed was maintained at the same temperature as the solubilization bed from 190 to 300°C then kept at 300°C when the solubilization bed is heated to 330°C. The purpose of this experiment was to prevent precipitation of lignin on the catalyst bed by maintaining the same temperature between the solubilization and catalyst beds. The liquid product yield and selectivities are shown in Table 3. The total carbon yield is 66-72% which is slightly lower compared to the data in Table 2. The main products are C_2-C_6 mono-alcohols and C_6-C_7 cyclic alcohols from cellulose. The ester selectivity is higher since the lower temperature catalyst bed cannot fully hydrogenate the methyl acetate from the acetyl groups in hemicellulose to ethanol. The selectivity to lignin dimers increases from 1.5% in bed 1 to 12.8% in bed 4 which is a similar pattern to what was observed in Table 2. However, the dimer selectivity is higher with the low temperature catalyst bed, possibly due to incomplete depolymerization of the soluble lignin. The catalyst activity slightly decreases over time as the C_8-C_{10} cyclic alcohol selectivity decreases from bed 1 to bed 4 (14.8% to 8.8%) while the phenolics selectivity increases by a similar amount (6.8% to 9.8%). The C_8-C_{10} cyclic alcohol selectivity

returns in bed 5 after regeneration of the catalyst showing that activity loss is reversible. A key difference between the two reactions is that the lignin yield in the 190-230˚C products is higher with the low temperature catalyst bed (21-41% vs. 13-19% lignin yield). It is possible that lignin does not deposit on the catalyst when the catalyst bed and solubilization are kept at the same temperature. The holocellulose yield of the 190-230˚C and 300-330˚C products is similar between the two reactions.

Table 3. Carbon yield and liquid product selectivity from SCM-DHDO of maple wood in a semi-continuous solubilization and packed bed reactor with six beds of maple wood. Catalyst regeneration after 4 beds of maple wood. Catalyst is kept at the same temperature as the solubilization bed at 190°C to 300°C.

Liquid Products	Bed 1	Bed 2	Bed 3	Bed 4	Bed 5	Bed 6
Total carbon yield (%C)	70.1	66.2	70.7	70.8	71.9	67.1
Lignin Yield ($\%C_{lignin}$)[a]	43.3	49.8	54.3	55.6	51.9	45.6
Holocellulose yield ($\%C_{holocellulose}$)[b]	87.3	76.8	81.2	80.6	84.6	80.8
Selectivities						
C_2-C_6 mono-alcohols	29.4	27.9	26.1	25.8	27.0	24.9
C_6-C_7 cyclic alcohols	20.2	19.4	18.8	16.1	19.3	18.6
Ethers and esters	11.2	12.8	12.6	13.3	13.2	14.7
Unknown C_2-C_6 alcohols, ethers, and esters[c]	15.2	10.6	12.6	14.2	12.3	15.2
C_8-C_{10} cyclic alcohols	14.6	14.5	12.0	8.7	12.3	10.5
Phenolics	6.7	7.8	7.3	9.7	6.1	5.8
Lignin dimers and trimers	2.8	7.0	10.6	12.1	9.8	10.2
Residual Biomass (wt%)	13.6	14.5	12.4	11.7	12.7	15.4
Unsolubilized cellulose (wt%)	8.4	8.1	7.0	5.3	7.4	9.1
Char and degradation products (wt%)	4.2	5.5	4.7	5.4	4.6	5.7
190-230°C carbon yield (%C)	15.4	18.0	20.8	24.3	17.6	18.7
Lignin yield ($\%C_{lignin}$)	21.0	28.5	35.3	40.7	27.8	29.7
Holocellulose yield ($\%C_{holocellulose}$)	11.8	11.4	11.5	13.8	11.1	11.7
300-330°C carbon yield (%C)	54.7	48.2	49.9	46.5	54.2	48.4
Lignin yield ($\%C_{lignin}$)	22.2	21.2	19.0	14.9	24.1	15.9
Holocellulose yield ($\%C_{holocellulose}$)	75.5	65.4	69.7	66.8	73.5	69.1

[a]mol C from cellulose products/mol C of hemicellulose and cellulose in the maple wood
[b]mol C from lignin products/mol C of lignin in the maple wood
[c]products that are observed in the GC and may be identified in the GC-MS but were not verified by standards

The gas products from the reaction are shown in Figure 8. The catalyst reforms a negligible amount of methanol at 190 and 230°C but once the reactor is heated to 300°C the amount of methanol reformed is similar to previous reactions. The catalyst deactivates slower with the multi-temperature bed compared to the previous reactions. The methanol reformed decreases from 28% for bed 1 to 25% for bed 4 and remains at 25% after 6 beds of maple wood. In comparison, in

Figure 6 the methanol reformed decreases from 28% for bed 1 to only 21% for bed 6. The improved stability of the catalyst is likely due to reduced coking from precipitation of solubilized lignin as the stream from the solubilization bed is heated to the catalyst bed temperature.

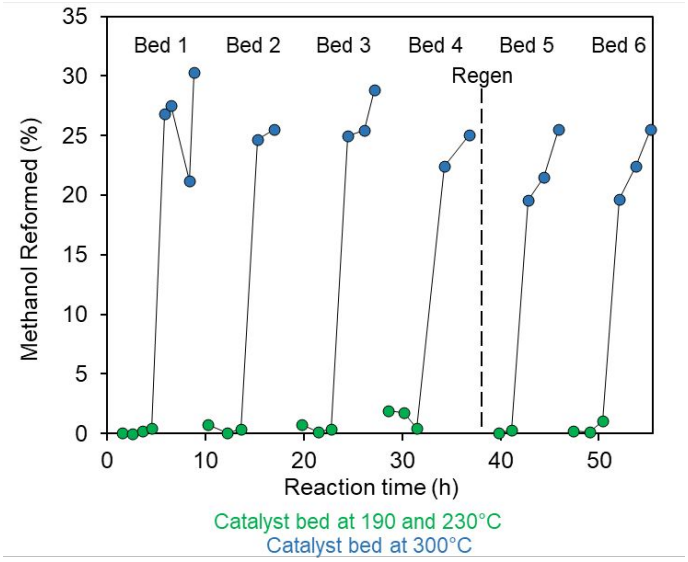

Figure 8. Methanol reformed from SCM-DHDO of maple wood in a semi-continuous solubilization and packed bed reactor with six beds of maple wood and catalyst regeneration after 4 beds of maple wood. Catalyst is kept at the same temperature as the solubilization bed at 190°C to 300°C

The molecular weight of the 190-230°C products from the 1st and the 4th (last before regeneration) were analyzed by GPC, shown in Figure 9. The 300-330°C products did not have enough high molecular weight compounds to analyze with GPC and are not shown here. The 190-230°C products from bed 1 are primarily monomers at approximately 170 Da with a smaller amount of dimers at 350 Da and trimers at 550 Da. As more beds of maple wood are converted the molecular weight of the products increases and more dimers and trimers are produced. The exact molecular weights of the 190-230°C and 300-330°C products from bed 1 and bed 4 were also analyzed by FT-ICR MS, shown in Figure 10 and 12. The FT-ICR MS of the 190-230°C products in Figure 10 shows similar molecular weights to the GPC, but with the main peak at the dimers rather than the monomers. In Figure 10a the main peak varies from 4-7 oxygen and 18-21 carbon

which is likely due to varying amounts of demethoxylation of the phenol ring or partial cleavage of the propyl tails of the dimers. In Figure 10b there are two dimer peaks which differ by 3-4 DBE which are likely partially hydrogenated and unhydrogenated dimers. In Figure 10d the ratio of hydrogenated to unhydrogenated dimers decreases which suggests the catalyst is losing hydrogenation activity from bed 1 to bed 4. In Figure 10b-d there is also an increase in the trimer peak at 30-32 carbon which agrees with the GPC in Figure 9 and may be due to catalyst deactivation decreasing the rate of hydrogenolysis of lignin linkages. The FT-ICR MS of the 300-330°C products in Figure 11a-d shows that the liquid products contain few high molecular weight species at this temperature. The absence of high molecular weight products after reaction suggests that either the degradation products observed in Figure 5e-h were converted to shorter products or they were deposited in the catalyst as char.

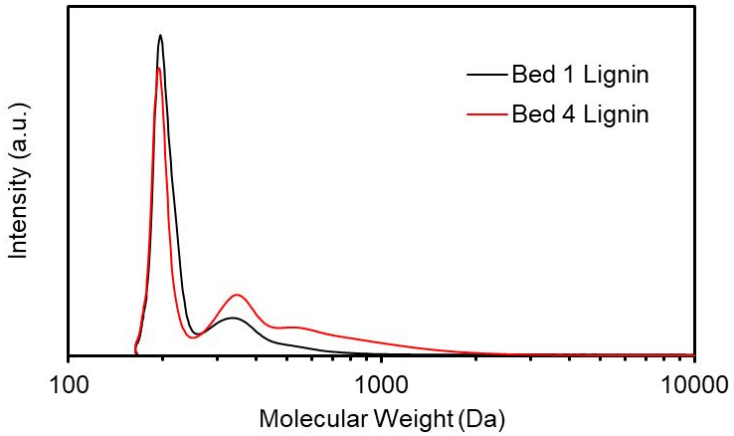

Figure 9. Gel permeation chromatography (GPC) of 190-230°C products from the 1st and 4th bed of maple wood during combined solubilization and conversion of maple wood in a flow through reactor over $CuMgAlO_x$ catalyst.

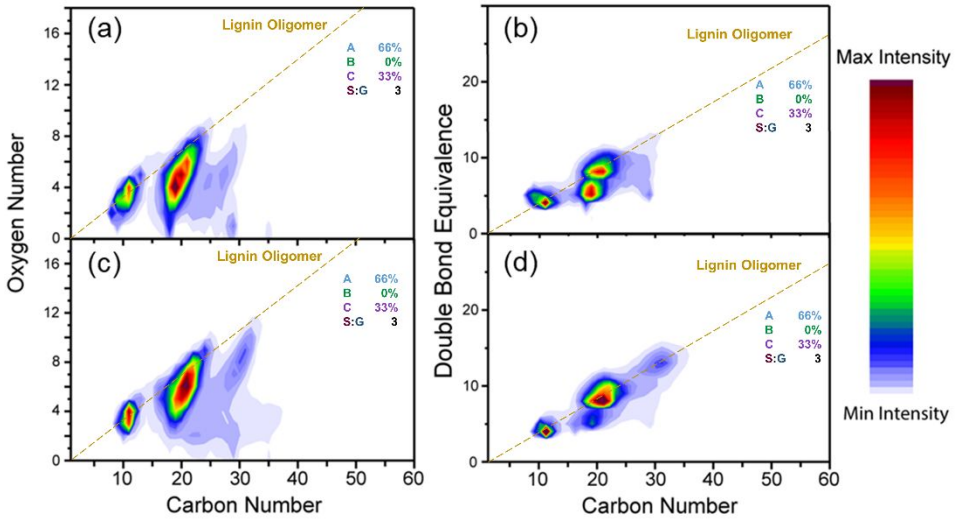

Figure 10. FT-ICR MS spectra of 190-230°C products after the 1st and 4th bed of maple wood during combined solubilization of maple wood in methanol and conversion with $CuMgAlO_x$. Bed 1 (a-b), bed 4 (c-d).

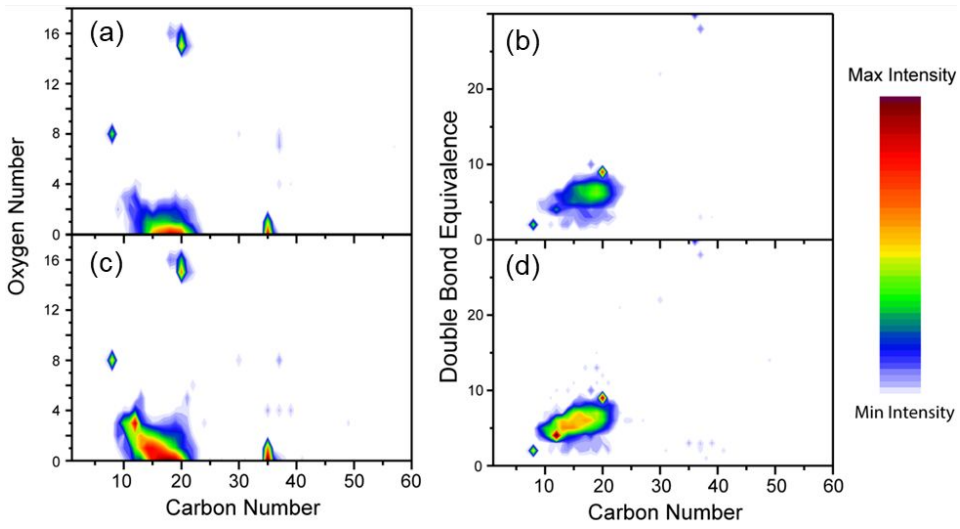

Figure 11. FT-ICR MS spectra of 300-330°C products after the 1st and 4th bed of maple wood during solubilization of maple wood in methanol and conversion with $CuMgAlO_x$. Bed 1 (a-b), bed 4 (c-d).

Characterization of catalyst after solubilization and conversion of maple wood

The catalyst from the reaction shown in Table 2 was characterized after bed 6 using ICP-AES, TPR, TPO, N_2O titration, N_2 physisorption, and STEM. The changes in the catalyst properties after reaction are shown in Table 4. The surface area of the catalyst decreases after reaction from 212 to 163 $m^2\ g^{-1}$. ICP of the catalyst shows that leaching of Cu is not occurring. The Cu dispersion from N_2O titration was 16.2% for the fresh catalyst and 8.7% for the spent catalyst which indicates that Cu sites on the catalyst are sintering during reaction. The average Cu particle size was calculated from the N_2O titration to be 5.2 nm for the fresh catalyst and 8.4 nm for the spent catalyst. TPO of the catalyst forms a small amount of CO_2 (2% of the carbon in the feed from beds 5 and 6) from burning of carbon on the catalyst surface. STEM images and particle size distributions of the fresh and spent catalyst are shown in Figures 12 and 13 respectively. All particle size distributions are averaged with at least 800 particles. The fresh catalyst is composed of small, well dispersed nanoparticles of Cu 1-4 nm in size. Very large particles were also detected (> 20 nm) which likely come from Cu that was not well integrated into the hydrotalcite during

synthesis and formed a separate crystal phase. The average particle size from STEM of the fresh catalyst is smaller than the particle size estimate from N_2O titration (3.5 nm vs. 5.2 nm). The difference is likely due to the larger nanoparticles which will be weighted more heavily towards average particle size for the N_2O titration than for STEM. The STEM of the spent catalyst has a bimodal distribution with a number of larger nanoparticles (6-13 nm) present in addition to the smaller (1-4 nm) particles observed in the fresh catalyst. The presence of larger nanoparticles confirms that the Cu is agglomerating possibly by an Oswald Ripening mechanism[52].

Table 4. Characterization of fresh and spent catalyst after reaction with maple wood with low temperature catalyst bed using TPR, TPO, N_2O titration, and N_2 physisorption.

	Fresh catalyst	Spent catalyst
BET surface area ($m^2\ g^{-1}$)	212	163
Cu/Mg/Al ratio (mol/mol/mol)	3/12/5[a]	3.2/11.7/5.1
N_2O uptake ($\mu mol\ g_{cat}^{-1}$)	30.3	16.5
Cu dispersion ($Cu_{surface}\ Cu_{bulk}^{-1}$)	16.2	8.7
Average Cu particle size (nm)	6.4	11.9
Carbon on catalyst (C% of feed)	NA	2
STEM of catalyst		
Average Cu particle size (nm)	3.5	5.7
Standard deviation of particle (nm)	6.4	10.9

[a]ratio of metals during synthesis

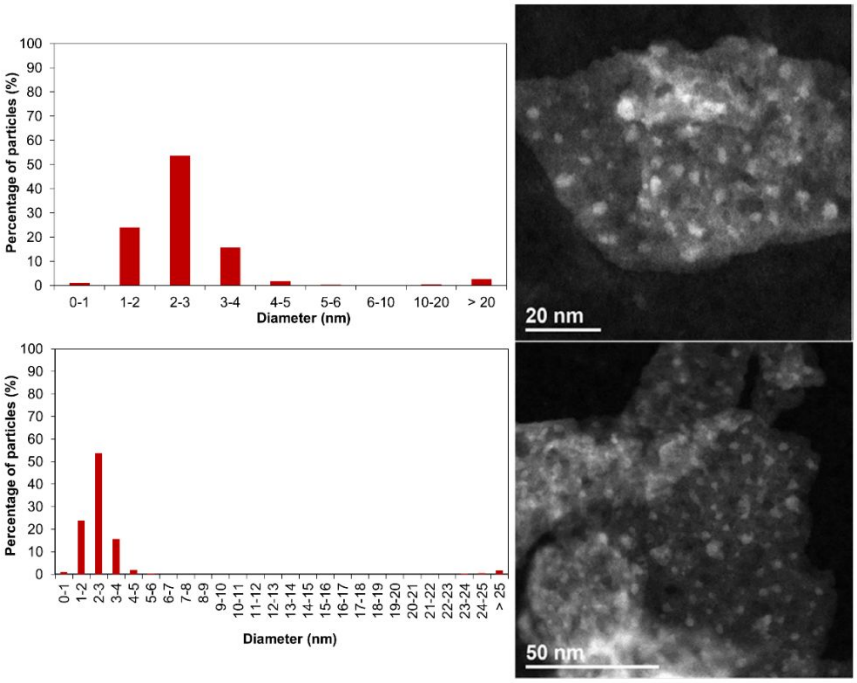

Figure 12. Particle size distributions and STEM images of fresh $CuMgAlO_x$ catalyst after being calcined and reduced in H_2.

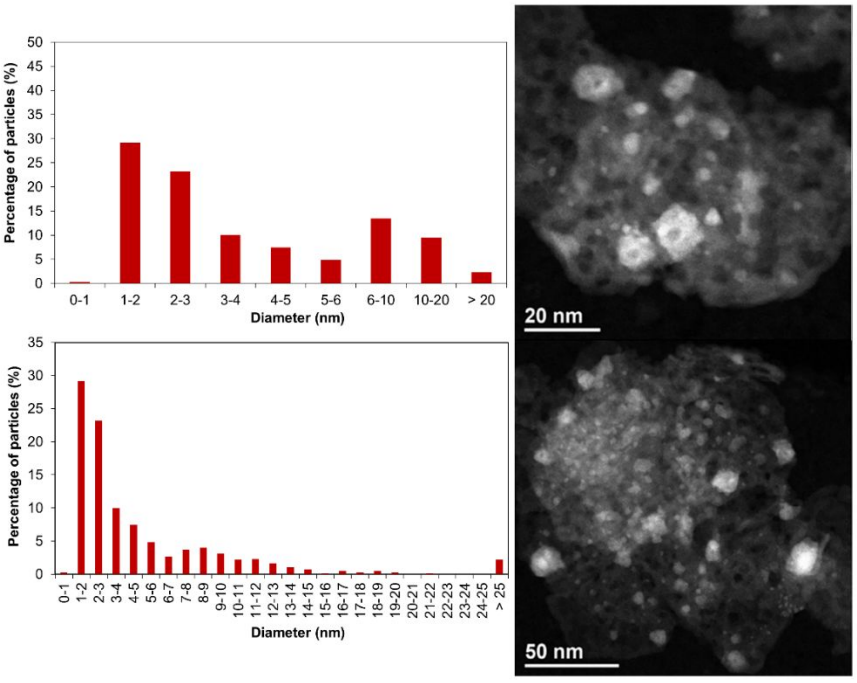

Figure 13. Particle size distributions and STEM images of spent catalyst from the reaction with the low temperature catalyst bed.

Batch reactions of maple wood at varying weight loading and solvents

Although combined solubilization and conversion in a packed bed was able to convert whole biomass semi-continuously, the concentration of biomass that is solubilized in methanol is low (~1 wt%), thus requiring an energy intensive separation process to remove the alcohol products from the methanol solvent. In addition, the yield from whole biomass in the flowthrough system, while high for a single step reaction, is still lower than what has been achieved using small batch systems which is often higher than 100% due to incorporation of methanol. In Table 5 we compare the batch reactions resulting from varying feed maple wood concentration (4-20 wt%) to the yields from the continuous reactor system. We also ran a two-step reaction at 10 wt% maple wood where additional biomass was added after reaction to simulate a reaction where part of the methanol could be replaced by the product alcohols. The yield of liquid products decreased with increasing weight loading from 104.9 %C at 4 wt% maple wood to 77.4% at 20 wt% maple wood. The decrease in yield at higher weight loading is due to a decreased holocellulose yield from, 133.1% to 86.2%. The two-step reaction with two charges of maple wood (10+10 wt%) has a slightly lower yield of 88.6 %C compared to the one-step 10 wt% yield of 92.9 %C. This reaction shows that product alcohols can partially replace methanol as the solvent during SCM-DHDO with minimal impact on yields. The carbon yield of liquid products from the batch reactor is higher at all loadings of maple wood compared to the flowthrough system. The lignin yield is only slightly lower for the flowthough system compared to the batch (50.1% vs. 60-67%) with similar yields of C_8-C_{10} cyclic alcohols, phenolics, and dimers. However, the flowthrough system has around 20-25% lower yields of C_2-C_6 mono-alcohols compared to the batch system. This lower yield is attributable due to differences between the two systems including: 1) the flowthrough system has

incomplete solubilization of cellulose and 2) the catalyst is separated from the biomass which decreases the rate of catalytic reactions that stabilizes intermediates.

Table 5. Carbon yield and individual product yields from batch and semi-continuous conversion of maple wood with SCM-DHDO.

	Batch Reactions (wt% maple wood)					Semi-continuous reaction
	4 wt%	7.7 wt%	10 wt%	20 wt%	10+10 wt%[a]	Low temp catalyst
Total carbon yield (%C)	104.9	95.3	92.9	77.4	88.6	68.9
Yield of holocellulose fraction (%C)[b]	133.1	115.9	113.3	86.2	102.4	82.0
Yield of lignin fraction (%C)[c]	60.8	63.1	61.1	63.1	66.8	48.3
Yields of product types						
C2-C6 mono-alcohols (%C)	44.7	40.2	38.0	28.6	35.0	18.8
C6-C7 cyclic alcohols (%C)	16.5	15.4	16.2	12.4	14.3	13.0
Ethers and Esters (%C)	6.8	4.4	5.1	2.7	4.6	9.0
Unspecified C2-C6 alcohols, ethers, and esters (%C)[d]	13.2	10.7	9.8	8.9	8.7	9.3
C8-C10 cyclic alcohols (%C)	13.2	14.2	13.8	10.8	13.3	8.4
Phenolics (%C)	3.2	2.4	2.4	3.6	3.1	5.0
Dimers (%C)	7.3	8.1	7.6	10.4	9.6	5.4

[a]10 wt% maple wood in methanol where makeup methanol and maple wood were added to the reactor after the first reaction to partially replace methanol with product alcohols as the solvent
[b]mol C from cellulose products/mol C of hemicellulose and cellulose in the maple wood
[c]mol C from lignin products/mol C of lignin in the maple wood
[d]products that are observed in the GC and may be identified in the GC-MS but were not verified by standards

Discussion and conclusions

Solubilization can be coupled with a fixed bed of $CuMgAlO_x$ catalyst to produce alcohols from maple wood semi-continuously. Solubilization of lignin takes place between 190°C and 230°C producing dimer and trimer lignin fragments with preserved partially preserved β-O-4, phenylcourmaran, and resinol linkages. Solubilization of maple wood at 300 and 330°C produces solubilized sugars as well as liquefaction products from degradation of the solubilized sugars. Conversion of the solubilized lignin and cellulose produces a mixture of linear and cyclic alcohols. Separating the solubilization and catalytic conversion of maple wood shows that the catalyst does not play a part in depolymerization of the biomass and that depolymerization occurs wholly through solvolysis. Additionally, this study shows that methanol can depolymerize the holocellulose portion of biomass in addition to the lignin fraction. The catalyst maintains

selectivity to mono-alcohols while converting multiple beds of maple wood. The catalyst is regenerable upon calcination and reduction but the Cu sites do undergo sintering due to an Oswald ripening mechanism. Maple wood can be converted in high weight loadings in batch reactors to a mixture of C_2-C_{10} alcohols with minimal loss in carbon yields. The carbon yield of maple wood from a flow reactor is lower than similar reactions in high pressure/high temperature batch reactors which we believe is primarily due to homogeneous degradation of sugars during solubilization.

Acknowledgements

This work was supported by ExxonMobil. The authors would like to thank the Magnetic Resonance Facility in the Chemistry Department of the University of Wisconsin– Madison for use of the Bruker Avance III 500 gifted by Paul J. Bender, the Center for Laser-Assisted NMR for use of the Bruker Avance III 600 (NIH S10 OD012245), and the DOE Great Lakes Bioenergy Research Center (DOE BER Office of Science DE-SC0018409), especially Dr. Steve Karlen, for their help analyzing the lignin and cellulose products. We acknowledge the NSF through the University of Wisconsin Materials Research Science and Engineering Center DMR-1720415.

References

1. Huber, G. W.; Iborra, S.; Corma, A., Synthesis of Transportation Fuels from Biomass: Chemistry, Catalysts, and Engineering. *Chemical Reviews* 2006, *106* (9), 4044-4098.
2. West, R. M., Kunkes, E.L., Simonetti, D.A., Dumesic, J.A., Catalytic conversion of biomass-derived carbohydrates to fuels and chemicals by formation and upgrading of mono-functional hydrocarbon intermediates. *Catalysis Today* 2009, *147* (2), 115-125.
3. Bond, J. Q.; Upadhye, A. A.; Olcay, H.; Tompsett, G. A.; Jae, J.; Xing, R.; Alonso, D. M.; Wang, D.; Zhang, T.; Kumar, R.; Foster, A.; Sen, S. M.; Maravelias, C. T.; Malina, R.; Barrett, S. R. H.; Lobo, R.; Wyman, C. E.; Dumesic, J. A.; Huber, G. W., Production of renewable jet fuel range alkanes and commodity chemicals from integrated catalytic processing of biomass. 2014.
4. Davis, R.; Tao, L.; Scarlata, C.; Tan, E. C. D.; Ross, J.; Lukas, J.; Sexton, D. *Process Design and Economics for the Conversion of Lignocellulosic Biomass to Hydrocarbons: Dilute-Acid and Enzymatic Deconstruction of Biomass to Sugars and Catalytic Conversion of Sugars to Hydrocarbons*; National Renewable Energy Laboratory: Golden, CO, 2015.

5. da Costa Sousa, L.; Chundawat, S. P. S.; Balan, V.; Dale, B. E., 'Cradle-to-grave' assessment of existing lignocellulose pretreatment technologies. *Curr. Opin. Biotechnol.* 2009, *20* (3), 339-347.
6. Ferrini, P.; Rinaldi, R., Catalytic Biorefining of Plant Biomass to Non-Pyrolytic Lignin Bio-Oil and Carbohydrates through Hydrogen Transfer Reactions. *Angewandte Chemie International Edition* 2014, *53* (33), 8634-8639.
7. Patil, S.; Lund, C., Formation and Growth of Humins via Aldol Addition and Condensation during Acid-Catalyzed Conversion of 5-Hydroxymethylfurfural. *Energy & Fuels* 2011, *25* (10), 4745-4755.
8. Rinaldi, R.; Jastrzebski, R.; Clough, M. T.; Ralph, J.; Kennema, M.; Bruijnincx, P. C. A.; Weckhuysen, B. M., Paving the Way for Lignin Valorisation: Recent Advances in Bioengineering, Biorefining and Catalysis. *Angew. Chem. Int. Ed.* 2016, *55* (29), 8164-8215.
9. Schutyser, W.; Renders, T.; Van den Bosch, S.; Koelewijn, S.-F.; Beckham, G. T.; Sels, B. F., Chemicals from lignin: an interplay of lignocellulose fractionation, depolymerisation, and upgrading. *Chem. Soc. Rev.* 2018, *47*, 852-908.
10. Renders, T.; Van den Bosch, S.; Koelewijn, S.-F.; Schutyser, W.; Sels, B. F., Lignin-first biomass fractionation: the advent of active stabilisation strategies. *Energy Environ. Sci.* 2017, *10* (7), 1551-1557.
11. Anderson, E. M.; Katahira, R.; Reed, M.; Resch, M. G.; Karp, E. M.; Beckham, G. T.; Roman-Leshkov, Y., Reductive Catalytic Fractionation of Corn Stover Lignin. *ACS Sustainable Chem. Eng.* 2016, *4* (12), 6940-6950.
12. Anderson, E. M.; Stone, M. L.; Katahira, R.; Reed, M.; Beckham, G. T.; Roman-Leshkov, Y., Flowthrough Reductive Catalytic Fractionation of Biomass. *Joule* 2017, *1* (3), 613-622.
13. Matson, T. D., Barta, K., Iretskii, A.V., Ford, P.C., One-Pot Catalytic Conversion of Cellulose and of Woody Biomass Solids to Liquid Fuels. *Journal of the American Chemical Society* 2011, *133* (35), 14090-14097.
14. Kozlowski, J. T.; Davis, R. J., Heterogeneous Catalysts for the Guerbet Coupling of Alcohols. *ACS Catal.* 2013, *3* (7), 1588-1600.
15. Eagan, N. M.; Kumbhalkar, M. D.; Buchanan, J. S.; Dumesic, J. A.; Huber, G. W., Chemistries and processes for the conversion of ethanol into middle-distillate fuels. *Nature Reviews Chemistry* 2019, *3* (4), 223-249.
16. Yin, W.; Venderbosch, R. H.; Bottari, G.; Krawzcyk, K. K.; Barta, K.; Heeres, H. J., Catalytic upgrading of sugar fractions from pyrolysis oils in supercritical mono-alcohols over Cu doped porous metal oxide. *Applied Catalysis B: Environmental* 2015, *166-167*, 56-65.
17. Wu, Y., Gu, F., Xu, G., Zhong, Z., Su, F., Hydrogenolysis of cellulose to C4–C7 alcohols over bi-functional CuO–MO/Al2O3 (M = Ce, Mg, Mn, Ni, Zn) catalysts coupled with methanol reforming reaction. *Bioresource Technology* 2013, *137*, 311-317.
18. Barrett, A. B.; Gao, Y.; Bernt, C. M.; Chui, M.; Tran, A. T.; Foston, M. B.; Ford, P. C., Enhancing Aromatic Production from Reductive Lignin Disassembly: in Situ O-Methylation of Phenolic Intermediates. *ACS Sustainable Chemistry & Engineering* 2016, *4* (12), 6877-6886.
19. Huang, X., Koranyi, T.I., Boot, M.D., Hensen, E.J.M., Catalytic Depolymerization of Lignin in Supercritical Ethanol. *ChemSusChem* 2014, *7* (8), 2276-2288.
20. Sun, Z.; Bottari, G.; Afanasenko, A.; Stuart, M. C. A.; Deuss, P. J.; Fridrich, B.; Barta, K., Complete lignocellulose conversion with integrated catalyst recycling yielding valuable aromatics and fuels. *Nature Catalysis* 2018, *1* (1), 82-92.

21. Galebach, P. H.; McClelland, D. J.; Eagan, N. M.; Wittrig, A. M.; Buchanan, J. S.; Dumesic, J. A.; Huber, G. W., Production of Alcohols from Cellulose by Supercritical Methanol Depolymerization and Hydrodeoxygenation. *ACS Sustainable Chem. Eng.* 2018, *6* (3), 4330-4344.
22. Galebach, P. H.; Thompson, S.; Wittrig, A. M.; Buchanan, J. S.; Huber, G. W., Investigation of the Reaction Pathways of Biomass-Derived Oxygenate Conversion into Monoalcohols in Supercritical Methanol with CuMgAl-Mixed-Metal Oxide. *ChemSusChem* 2019, *11* (23), 4007-4017.
23. McClelland, D. J.; Galebach, P. H.; Motagamwala, A. H.; Wittrig, A. M.; Karlen, S. D.; Buchanan, J. S.; Dumesic, J. A.; Huber, G. W., Supercritical methanol depolymerization and hydrodeoxygenation of lignin and biomass over reduced copper porous metal oxides. *Green Chem.* 2019, *21*, 2988-3005.
24. Elliott, D. C.; Biller, P.; Ross, A. B.; Schmidt, A. J.; Jones, S. B., Hydrothermal liquefaction of biomass: Developments from batch to continuous process. *Bioresour. Technol.* 2015, *178*, 147-156.
25. Scott, T.; Samaniuk, J. R.; Klingenberg, D. J., Rheology and extrusion of high-solids biomass. *Tappi* 2011, *10* (5), 47-53.
26. Anderson, E. M.; Stone, M. L.; Hülsey, M. J.; Beckham, G. T.; Román-Leshkov, Y., Kinetic Studies of Lignin Solvolysis and Reduction by Reductive Catalytic Fractionation Decoupled in Flow-Through Reactors. *ACS Sustainable Chem. Eng.* 2018, *6* (6), 7951-7959.
27. S., V. d. B.; Renders, T.; Kennis, S.; Koelewijn, S. F.; Van den Bossche, G.; Vangeel, T.; Deneyer, A.; Depuydt, D.; Courtin, C. M.; Thevelein, J. M.; Schutyser, W.; Sels, B. F., Integrating lignin valorization and bio-ethanol production: on the role of Ni-Al2O3 catalyst pellets during lignin-first fractionation. *Green Chem.* 2017, *19* (14), 3313-3326.
28. Zhu, G.; Qu, X.; Zhao, Y.; Qian, Y.; Pang, Y.; Ouyang, X., Depolymerization of lignin by microwave-assisted methylation of benzylic alcohols | Elsevier Enhanced Reader. *Bioresour. Technol.* 2016, *218*, 718-722.
29. Poirier, M. G., Ahmed, A., Grandmaison, J.L., Kaliaguine, S.C.F., Supercritical gas extraction of wood with methanol in a tubular reactor. *Industrial & Engineering Chemistry Research* 1987, *26* (9), 1738-1743.
30. Ishikawa, Y., Saka, S., Chemical conversion of cellulose as treated in supercritical methanol. *Cellulose* 2001, *8* (3), 189-195.
31. Minami, E., Saka, S., Comparison of the decomposition behaviors of hardwood and softwood in supercritical methanol. *Journal of Wood Science* 2003, *49* (1), 73-78.
32. Yamazaki, J., Minami, E., Saka, S., Liquefaction of beech wood in various supercritical alcohols. *Journal of Wood Science* 2006, *52* (6), 527-532.
33. Direct thermochemical liquefaction of microcrystalline cellulose by sub- and supercritical organic solvents. 2014, *95*, 175–186.
34. Pan, X.; Arato, C.; Gilkes, N.; Gregg, D.; Mabee, W.; Pye, K.; Xiao, Z.; Zhang, X.; J., S., Biorefining of softwoods using ethanol organosolv pulping: preliminary evaluation of process streams for manufacture of fuel-grade ethanol and co-products. *Biotechnol. Bioeng.* 2005, *90* (4), 473-481.
35. Erdocia, X., Prado, R., Fernandez-Rodriguez, J., Labidi, J., Depolymerization of Different Organosolv Lignins in Supercritical Methanol, Ethanol, and Acetone To Produce Phenolic Monomers. *ACS Sustainable Chemistry & Engineering* 2016, *4* (3), 1373-1380.

36. Zhao, X., Cheng, K., Liu, D., Organosolv pretreatment of lignocellulosic biomass for enzymatic hydrolysis. *Applied Microbiology and Biotechnology* 2009, *82*, 815.
37. Kabyemela, B. M.; Adschiri, T.; Malaluan, R. M.; Arai, K., Glucose and Fructose Decomposition in Subcritical and Supercritical Water: Detailed Reaction Pathway, Mechanisms, and Kinetics. *Ind. Eng. Chem. Res.* 1999, *38* (8), 2888-2895.
38. Peterson, A. A.; Vogel, F.; Lachance, R. P.; Fröling, M.; Antal, M. J.; Tester, J. W., Thermochemical biofuel production in hydrothermal media: A review of sub- and supercritical water technologies. *Energy Environ. Sci.* 2008, (1), 32-65.
39. Jacobsen, S. E., Wyman, C.E., Cellulose and hemicellulose hydrolysis models for application to current and novel pretreatment processes. *Applied Biochemistry and Biotechnology* 2000, *84* (1), 81-96.
40. Sasaki, M.; Kabyemela, B.; Malaluan, R.; Hirose, S.; Takeda, N.; Adschiri, T.; Arai, K., Cellulose hydrolysis in subcritical and supercritical water. *J Supercrit Fluid* 1998, *13* (1-3), 261-268.
41. Galebach, P. H.; Soeherman, J. K.; Wittrig, A. M.; Lanci, M. P.; Huber, G. W., Supercritical Methanol Depolymerization and Hydrodeoxygenation of Maple Wood and Biomass-Derived Oxygenates into Renewable Alcohols in a Continuous Flow Reactor. *ACS Sustainable Chem. Eng.* 2019, *7* (18), 15361-15372.
42. Sluiter, A.; Hames, B.; Ruisz, R.; Scarlata, C.; Sluiter, J.; Templeton, D.; Crocker, D. *Determination of Structural Carbohydrates and Lignin in Biomass*; NREL: 2008.
43. Galebach, P. H.; Thompson, S.; Wittrig, A. M.; Buchanan, J. S.; Huber, G. W., Investigation of the Reaction Pathways of Biomass Derived Oxygenate Conversion into Mono-alcohols in Supercritical Methanol with CuMgAl Mixed Metal Oxide. *ChemSusChem* 2018.
44. Macala, G. S.; Matson, T. D.; Johnson, C. L.; Lewis, R. S.; Iretskii, A. V.; Ford, P. C., Hydrogen Transfer from Supercritical Methanol over a Solid Base Catalyst: A Model for Lignin Depolymerization. *ChemSusChem* 2009, *2* (3), 215-217.
45. Macala, G. S., Robertson, A.W., Johnson, C.L., Day, Z.B., Lewis, R.S., White, M.G., Iretskii, A.V., Ford, P.C., Transesterification Catalysts from Iron Doped Hydrotalcite-like Precursors: Solid Bases for Biodiesel Production. *Catalysis Letters* 2008, *122* (3), 205-209.
46. Corilo, Y. E. *PetroOrg Software*, Florida State University: Tallahassee, FL, 2014.
47. Robinson, W. R. A. M., Mol, J.C., Characterization and catalytic activity of copper/alumina methanol synthesis catalysts. *Applied Catalysis* 1988, *44*, 165-177.
48. Cai, J.; Wu, W.; Liu, R.; Huber, G. W., A distributed activation energy model for the pyrolysis of lignocellulosic biomass. *Green Chem.* 2013, (15), 1331-1340.
49. Mansfield, S. D.; Kim, H.; Lu, F.; Ralph, J., Whole plant cell wall characterization using solution-state 2D NMR. *Nature Protocols* 2012, *7* (9), 1579-1589.
50. Kim, H., Ralph, J., Solution-state 2D NMR of ball-milled plant cell wall gels in DMSO-d6/pyridine-d5. *Organic & Biomolecular Chemistry* 2010, *8* (3), 576-591.
51. Zandvoort, I. V.; Koers, E. J.; Weingarth, M.; Bruijnincx, P. C. A.; Baldus, M.; Weckhuysen, B. M., Structural characterization of 13 C-enriched humins and alkali-treated 13 C humins by 2D solid-state NMR. *Gteen Chem.* 2015, *17*, 4383-4392.
52. Hansen, T. W.; DeLaRiva, A. T.; Challa, S. R.; Datye, A. K., Sintering of Catalytic Nanoparticles: Particle Migration or Ostwald Ripening? *Acc. Chem. Res.* 2013, *46* (8), 1720-1730.